AFRL-RH-FS-TR-2017-0022

Light Scatter in Optical Materials: Advanced Haze Modeling

Michael A. Guevara
William R. Brockmeier
Thomas K. Kuyk
Peter A. Smith
Engility Corporation

Barry P. Goettl
Brenda J. Novar
711th Human Performance Wing
Airman Systems Directorate
Bioeffects Division
Optical Radiation Bioeffects Branch

August 2017

Final Report for January 2016 to August 2017

Air Force Research Laboratory
711th Human Performance Wing
Airman Systems Directorate
Bioeffects Division
Optical Radiation Bioeffects Branch
JBSA Fort Sam Houston, TX 78234

NOTICE AND SIGNATURE PAGE

Using Government drawings, specifications, or other data included in this document for any purpose other than Government procurement does not in any way obligate the U.S. Government. The fact that the Government formulated or supplied the drawings, specifications, or other data does not license the holder or any other person or corporation; or convey any rights or permission to manufacture, use, or sell any patented invention that may relate to them.

Qualified requestors may obtain copies of this report from the Defense Technical Information Center (DTIC) (http://www.dtic.mil).

"Light Scatter in Optical Materials: Advanced Haze Modeling"

(AFRL-RH-FS-TR- 2012 - 0022) has been reviewed and is approved for publication in accordance with assigned distribution statement.

//SIGNATURE//
PATRICK SHORTER, Maj., USAF
Branch Chief
Optical Radiation Bioeffects Branch

//SIGNATURE//
STEPHANIE A. MILLER, DR-IV, DAF
Chief, Bioeffects Division
Airman Systems Directorate
711th Human Performance Wing
Air Force Research Laboratory

REPORT DOCUMENTATION PAGE

Form Approved
OMB No. 0704-0188

1. REPORT DATE *(DD-MM-YYYY)*	**2. REPORT TYPE**	**1. REPORT DATE** *(DD-MM-YYYY)*
03-31-2017	Final Report	January 2016 to August 2017

4. TITLE AND SUBTITLE

Light Scatter in Optical Materials: Advanced Haze Modeling

5a. CONTRACT NUMBER
FA8650-14-D-65190

5b. GRANT NUMBER

5c. PROGRAM ELEMENT NUMBER

6. AUTHOR(S)

Michael A. Guevara, William R. Brockmeier, Thomas K. Kuyk, Peter A Smith, Barry P Goettl, Brenda J. Novar

5d. PROJECT NUMBER

5e. TASK NUMBER

5f. WORK UNIT NUMBER
H08A

7. PERFORMING ORGANIZATION NAME(S) AND ADDRESS(ES)

Air Force Research Laboratory
711th Human Performance Wing
Airman Systems Directorate
Optical Radiation Bioeffects Division

Engility Corporation
4141 Petroleum Rd
Fort Sam Houston
TX 78234-2644

8. PERFORMING ORGANIZATION REPORT NUMBER

9. SPONSORING / MONITORING AGENCY NAME(S) AND ADDRESS(ES)

Air Force Research Laboratory
711th Human Performance Wing
Airman Systems Directorate
Directed Energy Bioeffects
Optical Radiation Bioeffects Branch

10. SPONSOR/MONITOR'S ACRONYM(S)
711 HPW/RHDO

11. SPONSOR/MONITOR'S REPORT NUMBER(S)
AFRL-RH-FS-TR-2017-0022

12. DISTRIBUTION / AVAILABILITY STATEMENT
Distribution A: Approved for public release; distribution unlimited. PA Case No: TSRL-PA-2017-0219

13. SUPPLEMENTARY NOTES

14. ABSTRACT

A simple scatterometer was constructed and used to make optical scatter measurements for four haze-standard samples. The scatter data were compared with independent measurements collected using a more sensitive and validated scatterometer and the results compared well. The scatter data were then imported into a modeling environment and modified using various built-in scatter editors. The scatter model showed a similar trend to the laboratory measurements, but produced significantly lower scatter values. Additional scatter measurements were made, and implemented with a surface scatter model and a volumetric scatter model, adjusted with "correction factors" to try to improve the match between the model and the laboratory measurements. To support validation of the applicability of the scatter model to human visual performance analysis, a 3D model of the optical set-up used in a study of the effects of optical scatter in the presence of glare on the visual acuity of human observers was developed. However, the version of the light scatter model was not considered to be sufficiently accurate that could allow generalizable representation of the laboratory measurements to support progression of this current model onto the validation step.

15. SUBJECT TERMS: Modeling and Simulation, Haze, Light Scatter, Scatterometer

16. SECURITY CLASSIFICATION OF:			**17. LIMITATION OF ABSTRACT**	**18. NUMBER OF PAGES**	**19a. NAME OF RESPONSIBLE PERSON**
Unclassified					Brenda Novar
a. REPORT	**b. ABSTRACT**	**a. REPORT**	Unclassified	27	**19b. TELEPHONE NUMBER (include area code)**
Unclassified	Unclassified	Unclassified			**210-539-8287**

Standard Form 298 (Rev. 8-98)
Prescribed by ANSI Std. 239.18

This Page Intentionally Left Blank

TABLE OF CONTENTS

TABLE OF FIGURES

LIST OF TABLES

1 INTRODUCTION

In military operations, the importance of protecting the eye from battlefield lasers has been recognized since the early 1980's. To that end, the US Air Force has developed laser eye protection (LEP) to mitigate the impact of laser illumination on the eye, the effects of which can range from temporary visual disruption to permanent eye damage. For aircrew, protection from the adverse effects of laser radiation is currently provided by passive optical filters that absorb and/or reflect laser light and are constructed in spectacle or visor formats. In addition to providing adequate laser eye protection, LEP must also be visually compatible with the operational environment. However, blocking laser light in the visible spectrum causes an unavoidable reduction in total amount of light transmitted by the filters and alters the incoming spectral content; this can cause unwanted visual effects such as reduced image contrast or changes in the appearance of colored stimuli. [1]

In addition to reduced transmission and spectral changes, another potential source of visual performance degradation is light scatter. When a user looks through protective eyewear, the scattering of light reduces the information content of the scene imaged resulting in degradation of vision. The appearance of images and scenes is observed as having blurring of edges and details, as well as an overall reduction in visual contrast. Depending on the amount of light scattering, the user's ability to perform a visual task or carry out a mission may be diminished. Haze is a term used to describe the scattering of light as it passes through a transparent material, resulting in poor visibility and/or glare. Haze can be inherent in the material, a result of the molding process, or a result of surface texture. Haze can also be a result of environmental factors such as optical material weathering or surface abrasion.

Haze is comprised of a single numerical value that is more specifically described as total integrated scatter. It is measured as the percent of transmitted light that is scattered so that its direction deviates more than a specified angle from the direction of the incident beam. The industry standard test method for optical materials specifies the deviation angle for haze measurement as light scattered more than 2.5°.[2] In practice, haze is measured by an instrument termed a "haze-meter" (Figure 1), consisting of a collimated light source illuminating the sample, an integrating sphere for collecting the scattered light, and a detector for measuring the amount of scattered light within the sphere. For decades, the US Air Force has specified the limits for light scattering in eyewear devices (protective eyewear, visors, and shields) in terms of haze. To preserve visual performance, current standards for aircrew LEP specify that the haze must be less than 3%.[3]

While haze is commonly used to define the overall magnitude of scattering within a protective eyewear device, it does not describe the scattering properties in detail. It has been known for some time that two optical devices having the same haze value may have quite different spatial distributions of that scattered light [4], but it was assumed the spatial characteristics of scattering were of secondary importance, so haze was used as the sole specification for scattering. However, some studies conducted within 711th Human Performance Wing, Airman Systems Directorate, Bioeffects Division, Optical Radiation Bioeffects Branch (RHDO), together with anecdotal reports, suggest that the 'single point' haze measurement correlates poorly with both visual performance metrics and with aircrew perceptions of haze, particularly in reflective LEP. In particular, two studies found that the relationship between the amount of haze in an LEP and visual

acuity, was not the same for the absorptive and reflective technology types when measured in the presence of an external glare source [5, 6]. For absorptive type LEP, the rate of decline in acuity with increasing haze paralleled that measured in a set of haze standards. For reflective LEP, the rate of acuity decline with increasing haze was greater compared to the haze standards or the absorptive LEP [6]. Furthermore, for reflective LEP a decrement in visual performance was observed in devices that met the Air Force's haze requirement.

Figure 1: BYK Gardner Haze Meter

More recently Kuyk et al., [7] reported that for reflective LEP, haze could not account for the decline in contrast acuity and contrast sensitivity with glare. This study measured angular scatter in the test articles, and showed that the cumulative (total) scatter beyond scatter angles greater than around 10° was a good predictor of the performance decline with glare These findings are supported by anecdotal reports of reflective LEP that meet the haze requirement, but being rejected in user tests, which suggest the possible involvement of factors unique to reflective technologies for which the haze measurement does not account.[8] The Kuyk et al., study is also consistent with limited field data that found a non-uniform distribution of scatter in reflective LEP, with relatively more scatter at higher scatter angles, was related to reduced acceptability in terms of subjective judgements of haze and visibility through the LEP.[8]

Taken together, these observations suggest that the traditional measure of integrating light scatter into a single value does not characterize optical materials in a way that allows a complete understanding of how light scatter effects image quality, visual performance and user acceptance. The purpose of the present effort was to develop a computational model that utilizes measurements of the angular distribution of light scatter in optical materials. This model could then be used to accurately represent the physical process of light scattering, and, with the incorporation of the scatter model, allow prediction of light scatter effects on the sensed visibility of visual stimuli posed to human observers.

2 METHODS

2.1 Overall approach

Our initial approach consisted of making cursory measurements of the angular scattering characteristics of BYK haze standards (1, 5, 10 and 20% haze) within the RHDO laboratory, importing these data into a Computer Aided Design (CAD) environment, and attempting to replicate the laboratory measurements *"in silico"*. Modifications were later made to the laboratory measurement system to provide higher resolution and more accurate measurements of light scatter. Independent scatter measurements were also made by two external agencies.

The initial CAD steps involved setting up the measurement system geometry (light source, optical sample and detector) within the three-dimensional (3D) CAD environment. This concept included incorporating the measured light scattering functions into the optical properties of the model of the optical sample. This provided a validation step, where the model predictions of light scatter could be compared with the actual scatter measurements. Since there are several scatter models available in the modeling environment, this step was used to find which approach provided the best correlation between the laboratory measurements and the simulation results. The next phase involved constructing scenarios within the modeling environment, applying the light geometry used in the Kuyk et al [7] experimental study concerning the effect of scattered light on visual function, so that legibility and visibility models of human vision could be used to estimate the effect of scatter on visual performance and allow comparisons of the model with the empirical results.

2.2 Scatter measurements

The bidirectional scattering distribution function (BSDF) is a radiometric characterization of the scatter of optical radiation from a surface as a function of the angular positions of the incident and scattered beams. By definition, it is the ratio of the scattered radiance to the incident irradiance, and the unit is inverse steradians (sr^{-1}). The term bidirectional reflectance distribution function (BRDF) is used when specifically referring to reflected scatter. Likewise, bidirectional transmittance distribution function (BTDF) refers to light scatter transmitted through a material. Taken together, the BTDF and the BRDF make up the complete BSDF. For the purposes of modeling the effect of eyewear scatter on visual performance, only the BTDF portion is of current interest.

2.2.1 RHDO scatter measurements

For the in-house scatter measurement system, a computer-controlled stage was used to rotate an illuminated optical sample and sweep the light scattered by the sample across a light detector (10 mm diameter silicon photodiode) located 1000 mm from the sample. A partially-collimated probe beam of 532 nm laser light was used to illuminate the sample at a fixed angle of incidence, normal (perpendicular) to the surface (Figure 2). The laser light was focused onto an optical fiber and exited at the end nearest the sample via a collimator. The use of an optical fiber system allowed the sample and beam to be rotated together in a fixed geometry (Figure 3 and Figure 4). The beam size was approximately 10 mm in diameter at the sample, with a total power of about 13 mW. The angular distribution of the scattered light was measured by rotating the beam and sampling incrementally about a vertical axis, through a 90° angle from the beam direction.

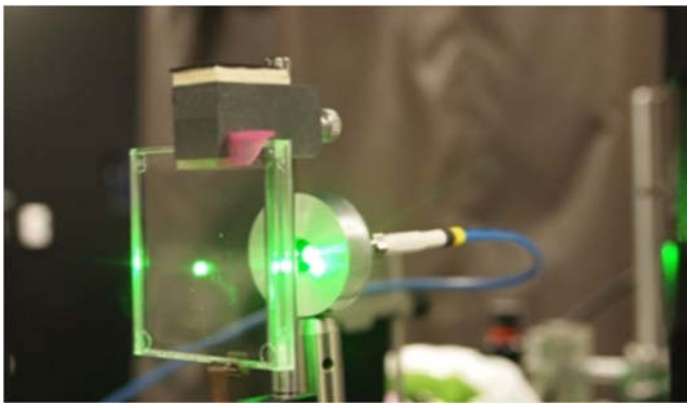

Figure 2: Sample under laser illumination for angular scatter measurements

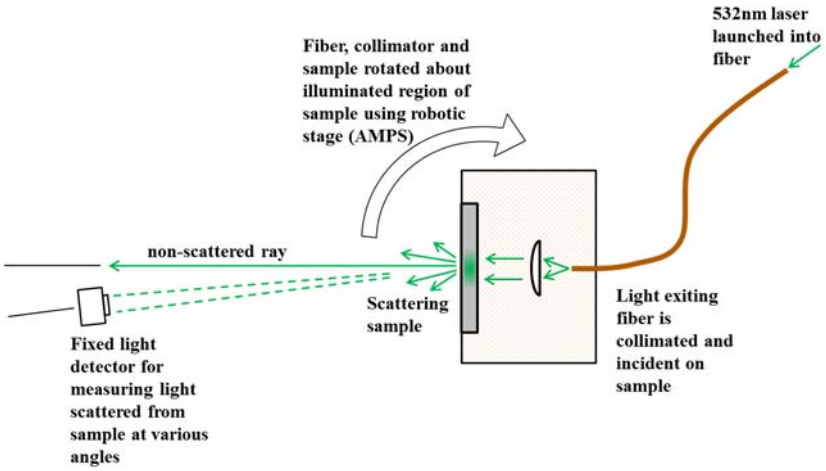

Figure 3: Scatter measurement system at a small scatter angle

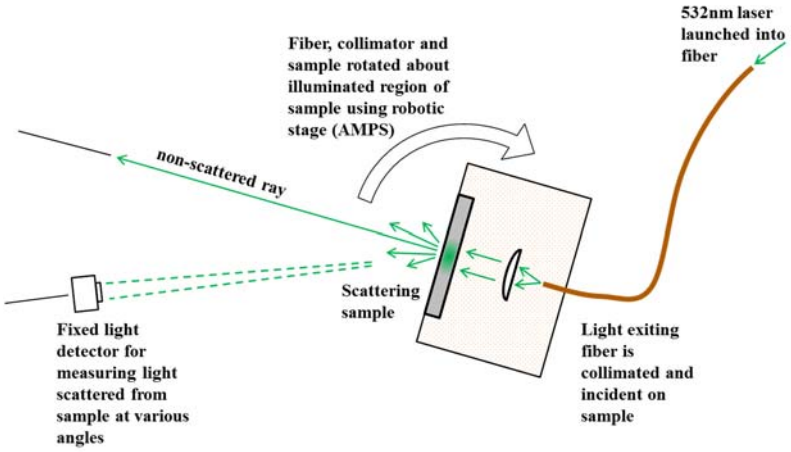

Figure 4: Scatter measurement system at a large scatter angle

The capabilities of the scatter measurement system were found to be limited due to light leaks, general scattered light present in the laboratory, and low laser power, all of which served to reduce the signal-to-noise ratio. This resulted in a measurement floor equivalent to a low-end of scattered light of about 5×10^{-4} sr^{-1}, which is about two orders of magnitude above that of a dedicated scatterometer. The system was improved by fixing both the sample and laser beam in space, and using the rotation system to rotate the detector around the sample, thereby sweeping it through the field of scattered light (Figure 5). The detector was attached to the rotation system by an aluminum rod, holding the detector at a constant 405 mm radius from the sample. This shortened distance increased stability and the intensity of the scattered light falling on the detector, but it also decreased the angular resolution of the measurements. The fact that the sample and beam were now fixed in space also allowed the laser beam to be directly incident on the sample, with no flexible optical fiber required, resulting in an increase in delivered laser power by a factor of ten. Overall, these modifications dropped the measurement floor to an equivalent of 3.5×10^{-5} sr^{-1}, an improvement of more than an order of magnitude.

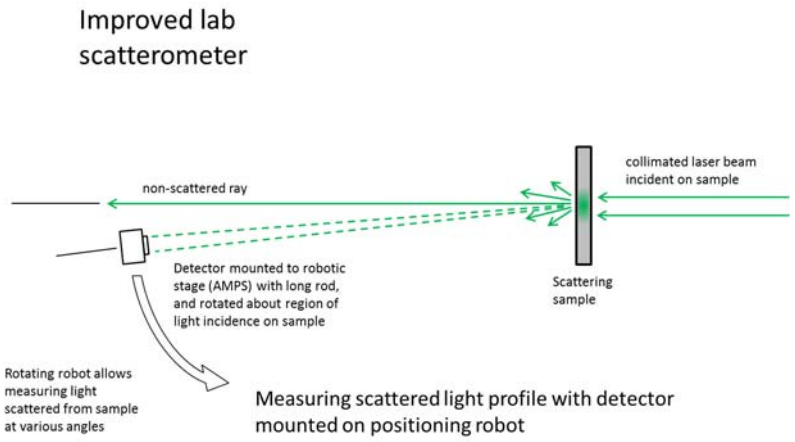

Figure 5: Improved RHDO scatter measurement system

2.2.2 Nanohmics scatter measurements

To provide a cross-comparison of the scatter measurements taken in the RHDO laboratory, the haze standards were sent to an independent laboratory (Nanohmics Inc, Austin TX), where scatter measurements were made with a different, more robust scatter measurement system capable of producing higher resolution data. The Nanohmics scatterometer is a versatile instrument capable of measuring reflected and transmitted light scatter of various optical samples, at different wavelengths, and with selectable source and analyzer polarizations.

For measurement of the haze samples, the scatterometer was configured to emit a spatially-filtered laser beam at a wavelength of 532 nm. The laser beam travels through the center of the sample stage, and converges to a focal point at the locus of the detector (Figure 6). A variable aperture allows adjustment of the source beam size at the position of the sample. High-quality optical components are used to ensure a well-defined, truncated Gaussian profile beam with a

very small amount of light outside the beam. Polarizers and retardation plates inside the source optics box allow the source polarization to be changed. A small sample of the source radiation is collected and sent to a second detector to provide a signal to normalize the primary detector signal to any fluctuations in source intensity.

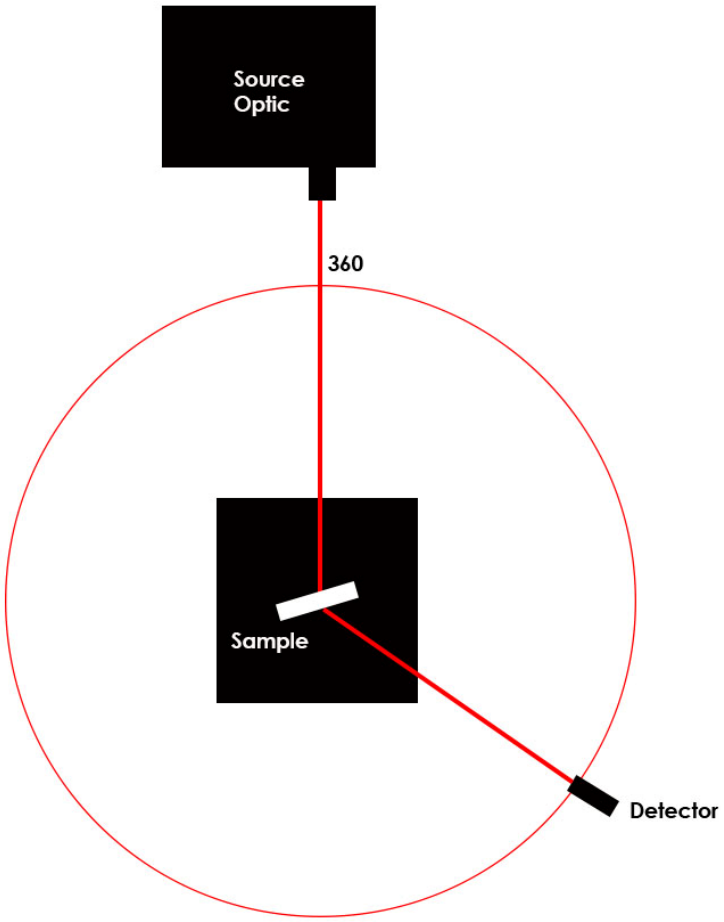

Figure 6: Schematic diagram of Nanohmics scatter instrument

The detector assembly is mounted on the end of an adjustable arm that can rotate 360° around the sample, with the detector rotation defining the plane of measurement. The detector has an adjustable aperture, a spectral bandpass filter centered at the source wavelength, a polarization analyzer, and provision for optical attenuation via individually calibrated neutral density filters.

2.3 Modeling light scatter

The light scatter modeling environment consisted primarily of SolidWorks™ (SW) and OptisWorks™ (OW), both of which are developed by Dassault Systemes in France. SW is a 3D CAD design tool, while OW is an add-in for SW that provides a light simulation solution based on a physical model fully integrated into the CAD software suite. The OW add-in provides

different scatter models (Editors), which are used to simulate different types of light scatter. Three of these editors were evaluated and used in support of this modeling effort: the Simple Scattering, Advanced Scattering (Volumetric) and the User Material editors.

After a comprehensive evaluation, it was determined that the User Material Editor (UME) would be the most appropriate and effective method to simulate the light scattering for each of the haze standards within the CAD environment. The UME is designed to build complex materials, which can be stored in a materials database and later imported into the scatter model. Material files were developed using this editor for each of the BYK haze standards and stored within the materials library database. The primary decision for selecting this editor was centered on the types of data collected in the laboratory and how it correlated to the input parameters provided by the UME. As a result, the data could be input by defining the scattering efficiency according to the scattering angle and the relative intensity. Once the material file was developed it was imported into the model and defined as a Face Optical Property, also referred to as a Surface Quality (material).

The initial modeling phase involved constructing a 3D assembly model within the SW CAD environment that consisted of three components, a Surface Source, a haze sample and an illuminance sensor. The assembly model was designed to represent the laboratory setup for the RHDO scatterometer with dimensions taken from the physical setup defined within the model.

The Surface Source is an OW feature that is used to define the light emission properties of the light source in the model. For the simulation, the light emission parameters for the Surface Source were defined to propagate light at a wavelength of 532nm with a Gaussian intensity distribution, at a power of 13 mW. An Illuminance Sensor was defined at a distance 405 mm from the front surface of the sample. Reference geometry is drawn on this location which establishes the origin and the XY direction. The Illuminance Sensor is a light detector that computes the illuminance/irradiance produced by the OW simulation of the light from the Surface Source passing through the haze sample. The haze sample model is a 3D component constructed from the physical measurements of the sample. This component provides the surface in the model to which the material files, previously developed with the UME, are assigned.

Once the parameters for each of the components were established and fixed into position, how they would move with respect to each was then defined. The assembly model was configured so that the haze sample and light source remained fixed relative to each other, with their faces parallel to each other as the sample rotates. The detector remained in a fixed position and did not move as the sample and source rotated (Figure 7). The configuration was set up to allow the haze sample to rotate incrementally from 0 to 45° in 2° steps. Multiple configurations were set up in OW, and the simulations were run sequentially, which made the process of data collection quick and efficient. These configurations are predefined positions within the model that allow the model to move to a specific position as opposed to manually manipulating the model.

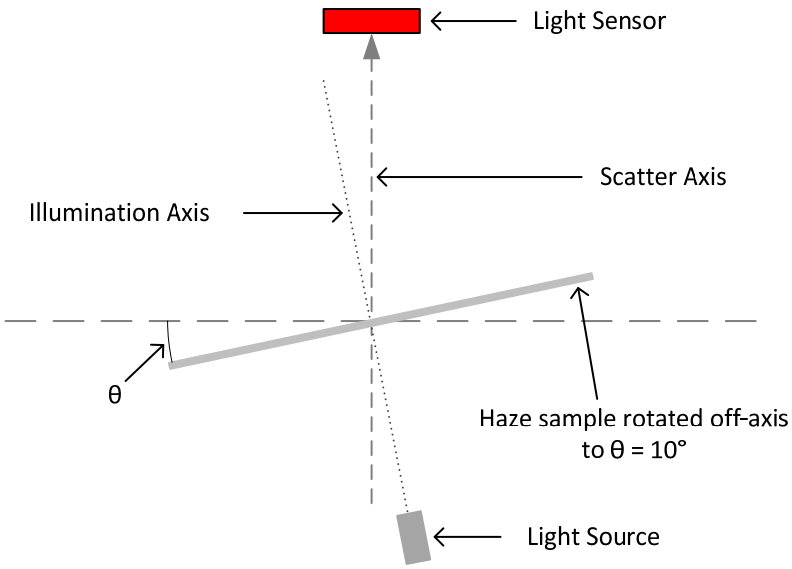

Figure 7: Schematic diagram for OW scatter simulations showing light source, optical sample and light sensor

The results from the initial simulations using the material file developed from the laboratory scatter data produced results that were inconsistent with measurements taken in the laboratory, although they showed a similar trend. These differences were attributed to the data transformations being done within the scatter model of OW, but because of the proprietary restrictions of the OW BSDF file format, information about the file structure and the calculation algorithms were not available. Repeated attempts to compensate for these transformations were made by editing the input data file, but these modifications were unsuccessful.

The process of importing a scatter file is an essential first step in validating that the model could accurately reproduce laboratory measurements. In order to progress past this step, it was decided to obtain and use an Optis generated data set as the material file. To facilitate this, the 5% BYK haze sample was sent to Optis North America so measurements could be taken using their Optical Material Scanner (OMS4) system. This device is a goniometer-based measurement system designed to collect empirical scattering data for optical samples and produce native OW BSDF material files. Optis used the OMS4 to measure the BSDF for the 5% haze standard. The resultant material file was imported into the existing model and applied as a Surface Quality material. Simulations were then performed using the methods described previously.

The final part of the project involved modeling the effects of light scatter and glare produced from optical materials on human visual performance, and compare these results with actual experimental data from human observers [5]. To achieve this, the light geometry of the laboratory study was established in OW.

In the human study, visual acuity was assessed with the Regan Contrast Acuity Test with subjects viewing the test charts through optical materials with different scatter properties that was performed with or without a glare source present. The first step was to construct the optotypes

from the Regan contrast acuity chart within SW, and then use them as visual targets in simulations of the effects of scattering by the optical samples.

The Regan test consists of five charts. Each chart is made up of six to eight lines of black letters on a white background. The letters on a line are of the same size with the top line containing the largest letters and size decreasing for each line reading down the chart. All letters on a chart have the same contrast, and the five charts have contrast levels of 96, 50, 25, 11, and 4% (Figure 8). The letter contrast levels are achieved by using dark letters of different reflectivity on a bright white backgrounds of constant reflectivity. [9]

As a component of the 3D model, a digital version of the Regan Chart was made. For this, each of the characters for the first line of the chart were constructed within the model. These were then analyzed to determine the dimensional scaling factor for the letters from line to line. A single line of letters was produced as a digital model in bitmap image format to facilitate its use as a display source in OW. The resolution of the bitmap was chosen to be high enough to allow sufficiently precise simulations, without unduly increasing simulation times.

In the laboratory, the charts are illuminated by a fixed light source that results in known luminance levels for the dark characters and the white background. Rather than modeling the illuminants as emissive sources, the digital models were set up to produce the specified luminance levels for the characters and background directly. This test was done by setting up the charts as “Display Sources” in OW. A Display Source is a six-layered model consisting of three layers or channels of red, green and blue (RGB) light emission overlaid by three RGB layers or channels of light modulation. The emission element is a rectangular planar emission surface specified for spectral content and maximum luminance. The modulation element uses a bitmap image to modify (attenuate) the amplitude of the light passing through each pixel of the image. Each of the three channels operates independently and then the total light for each pixel is summed at the output. While the Display Source allows arbitrary control of the three RGB channels and detailed spectral content, the Regan Charts are black/gray/white so a monochromatic light scheme was chosen by making each of the RGB channels equivalent. To change the Regan letter/line size, the bitmap image size of the Display Source was simply scaled to the appropriate dimensions.

The digital bitmaps used in the OW simulations were configured to reproduce the contrast levels accurately. Within OW, the primary purpose of the Display Source module is to simulate digitized displays and provide an attenuation function that applies a gamma function rather than a simple linear relationship to the pixel value. This condition meant that the chart contrast models could not be produced accurately using values that were linearly related to the contrast. To create this condition, the appropriate values were calculated from the gamma function, and were applied to the character pixels in the various contrast bitmap images to produce the correct luminance, and hence contrast, values.

ZRDOVCNS

Figure 8: Digital model of contrast acuity charts at 96 (top) and 11% contrast (bottom)

In the model, the human observer was represented as an OW sensor, which was defined at a distance of 6 m away from the characters. This positional set-up allows the viewing distance specified for the Regan test. In OW a "Luminance Detector" sensor may be set up to represent a human observer within the 3D model. The detector is pyramidal in shape, with the apex defining the location point of the observer and the rectangular base defining the horizontal and vertical fields of view (FOV) for the observer (Figure 9). The base of the pyramid can be thought of as the "window" through which the observer views the scene.

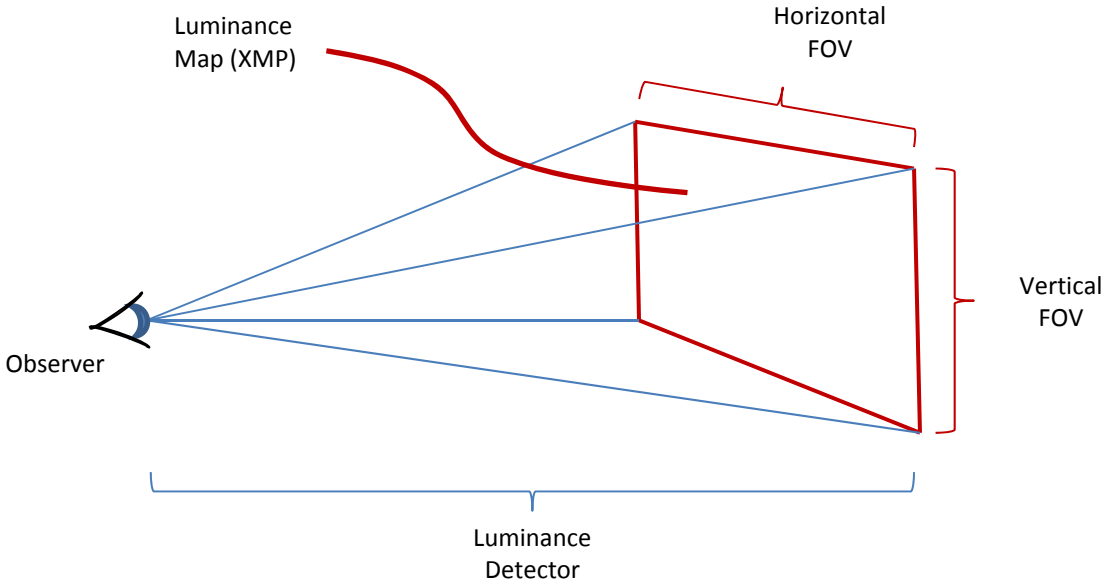

Figure 9. Luminance detector showing its field of view.

When the Luminance Detector is set up, its geometry can be arbitrarily specified to define specific vertical and horizontal FOVs and the desired spatial resolution. When an OW simulation is run, the luminance of each element of the scene apparent to the observer is mapped to the corresponding pixels of a specialized bitmap-image (.XMP, or extended image map), also located within the rectangular base of the Luminance Detector pyramid. Once the XMP has been produced by the simulation, the luminance data can be directly displayed and viewed as a visual analog of what the observer would see, or the data may be numerically operated to determine minimum, maximum or averages of arbitrary regions of interest within the field of view. The Luminance Detector, which

collects both photometric and radiometric measurements, computes radiant intensity ($W \cdot sr^{-1}$) and generates a "XMP Basic Map" that is used within the OW Human Vision Lab analysis tool. The Human Vision Lab is the built-in vision model designed to perform predictive analyses of lighting and illumination simulations.

The human study used a Brightness Acuity Tester (BAT) to induce glare while performing visual tasks (Figure 10). The BAT is a clinical tool that provides a wide field-of-view glare source to assess functional visual acuity in bright light conditions. The BAT is comprised of a diffuse-white near-hemispherical bowl, illuminated by a bright filament bulb near its upper perimeter. The illuminated concave surface of the bowl is presented toward the eye and brought close enough that its edge touches the face (at the cheek and brow). The eye is shielded from direct illumination by the bulb with a small baffle, the inner surface of which reflects backside light from the bulb back toward the bowl. The center of the bowl has a clear aperture cut through it, allowing the eye an unobstructed field of view near the central axis, with an included cone angle of about 16°. The glare source extends out to a field of about 132°. The illumination level of the BAT averages about 1000 $cd \cdot m^{-2}$. To include this tool in the modeling environment, a 3D model of the BAT was developed (Figure 11), and this model was integrated into the assembly model.

Figure 10. The Brightness Acuity Tester

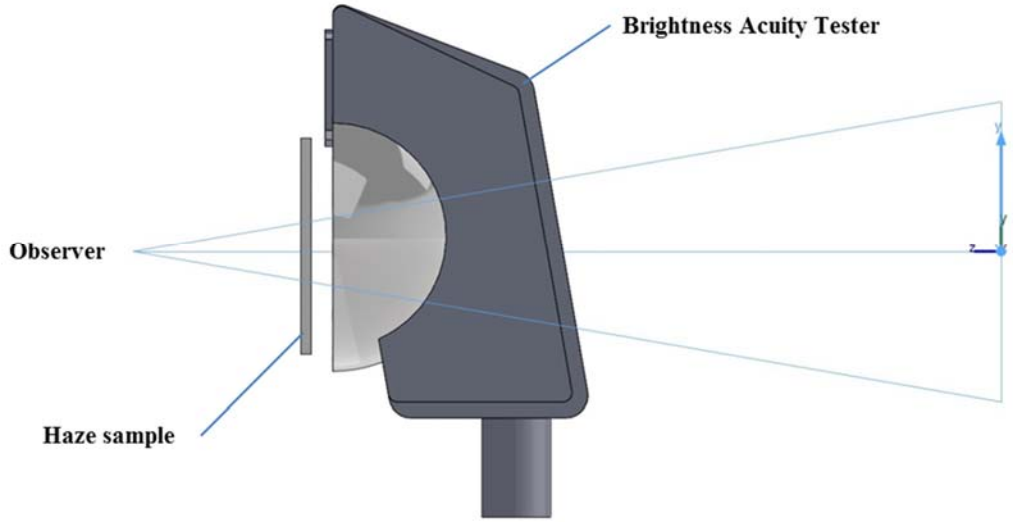

Figure 11. Right view of the assembly model showing observer position looking through haze sample and BAT to Regan chart (distances not to scale).

3 RESULTS

3.1 Light scatter measurements

Plots of the RHDO-measured light scatter functions for the four Gardner haze standards (1, 5, 10, and 20%) are shown in Figure 12, relative to the incident beam axis (0°). As expected, the amount of scatter increases with increasing haze level, and the scatter fraction is seen to decrease with increasing angle. The functions for 10 and 20% haze are roughly parallel. However, at large angles (~60°) the curves for the 5% and 10% samples converge around the same scatter fraction, despite the differences in total integrated scatter.

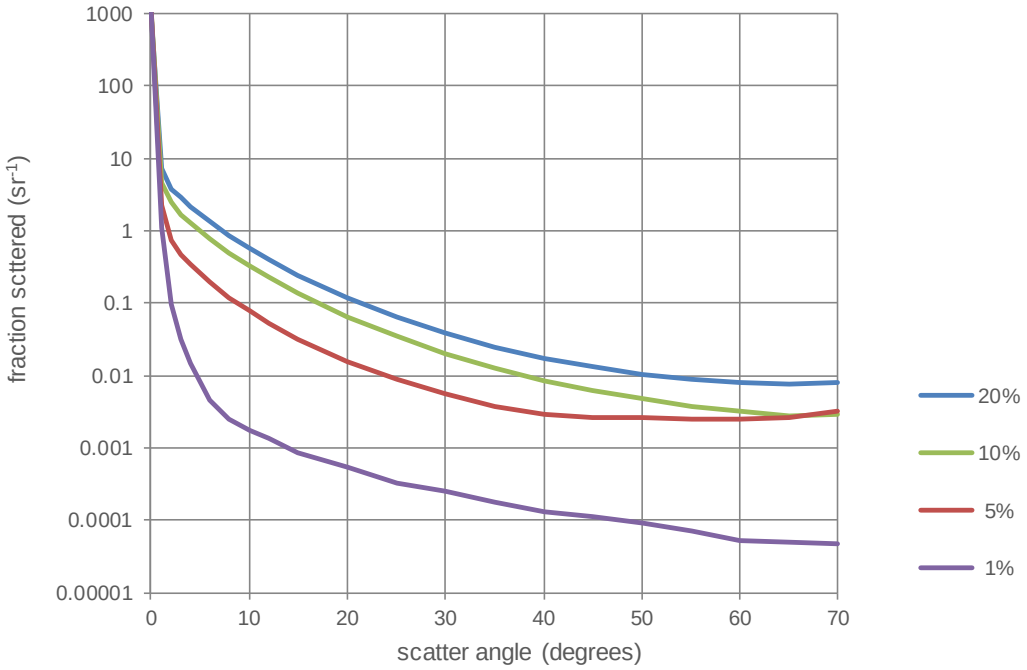

Figure 12. RHDO scatter measurements for 1, 5, 10, 20% haze standards

Plots of the Nanohmics-measured scatter functions for the same four Gardner haze standards as used in the RHDO scatter measurements are shown in Figure 13. Although Nanohmics measured scatter for perpendicular (S) and parallel (P) source polarization, only those for the P-polarization are shown – those for S-polarization were very similar. For reference, Figure 13 also shows the RHDO scatter measurements - the results correlate closely with the Nanohmics measurements. The Nanohmics scatter curves appear to run in parallel to a greater extent than the RHDO measurements, exhibiting better separation at large angles. Also, the Nanohmics data curve for the 1% haze sample shows much more scatter than the RHDO measurements. These differences are most likely due to the higher sensitivity and resolution of the Nanohmics system. Taken together, the laboratory-measured scatter functions indicate that four haze samples exhibit similar angular dependencies, while differing in the magnitude of scatter.

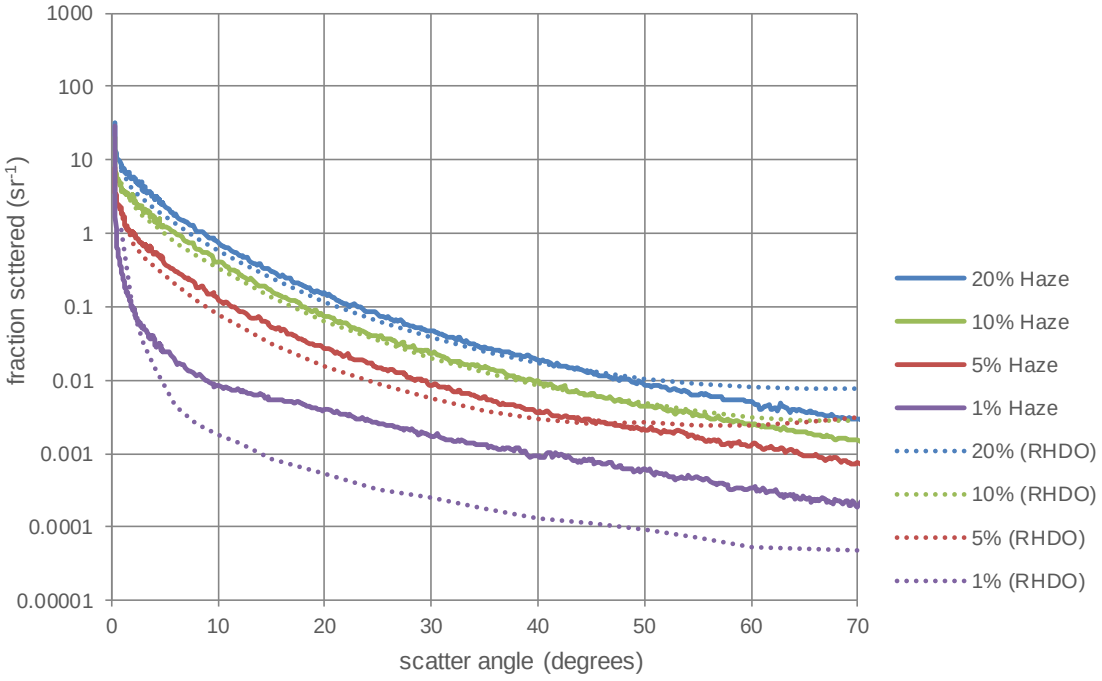

Figure 13. Comparison of Nanohmics scatterometer measurements (solid lines) with the RHDO measurements (dotted lines) for the 1, 5, 10 and 20% haze standards

3.2 Modeling results – Light scatter

Comparisons of the laboratory measured scatter for the 5 and 20% haze standards with the OW simulation data utilizing the RHDO generated material files is shown in Figure 14. Although the plots indicate a similar trend in scattering with respect to incident angle, the OW simulation shows significantly lower levels of scatter, and very little separation between the two samples. Consultation with subject matter experts at Optis suggested that the application of an empirically-derived correction factor could be used to improve the fit.

In making measurements of the 5% haze sample with the OMS4, Optis experts commented that since the haze sample is only slightly scattering, it may be too transparent to deliver a reliable BSDF measurement. Typically the instrument is used to measure scatter in materials that have a significant amount of diffuse scattering. Nonetheless, the measured BSDF file was used in two simulation approaches, applying it in OW as a "Surface Scatterer" and as a "Volumetric Scatterer". Comparisons of the results using these two simulation approaches, after the application of correction factors, are shown together with the laboratory measured scatter Figure 15. At small angles (<7°), the surface scatter approach appears to provide a better fit, while the volume scattering approach seems to be better for larger angles.

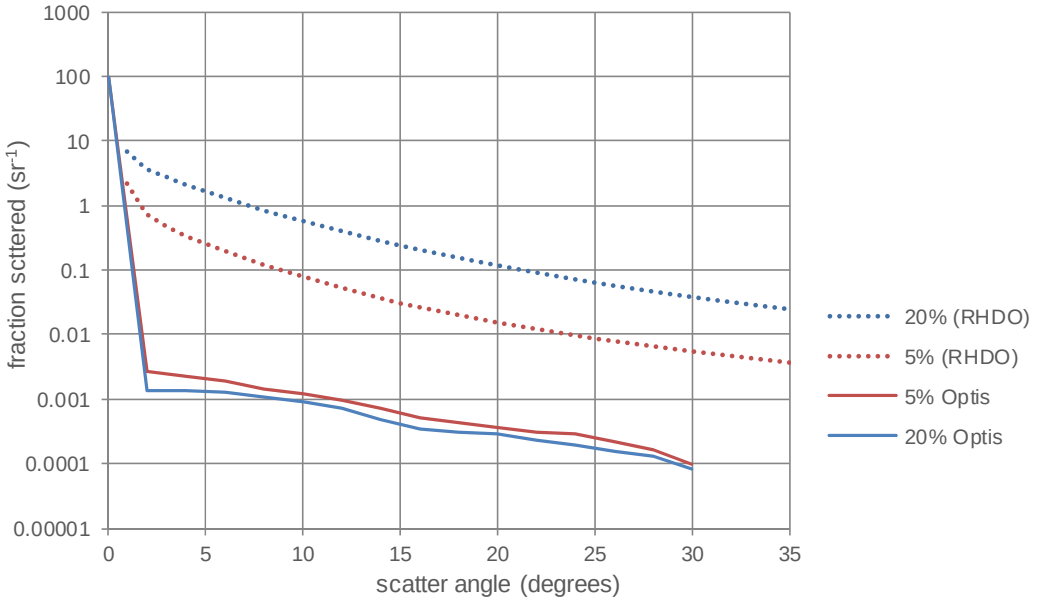

Figure 14. Optis simulation results (solid lines) compared to RHDO Laboratory measurements (dotted lines) for the 5% and 20% haze standards (RHDO BSDF material file)

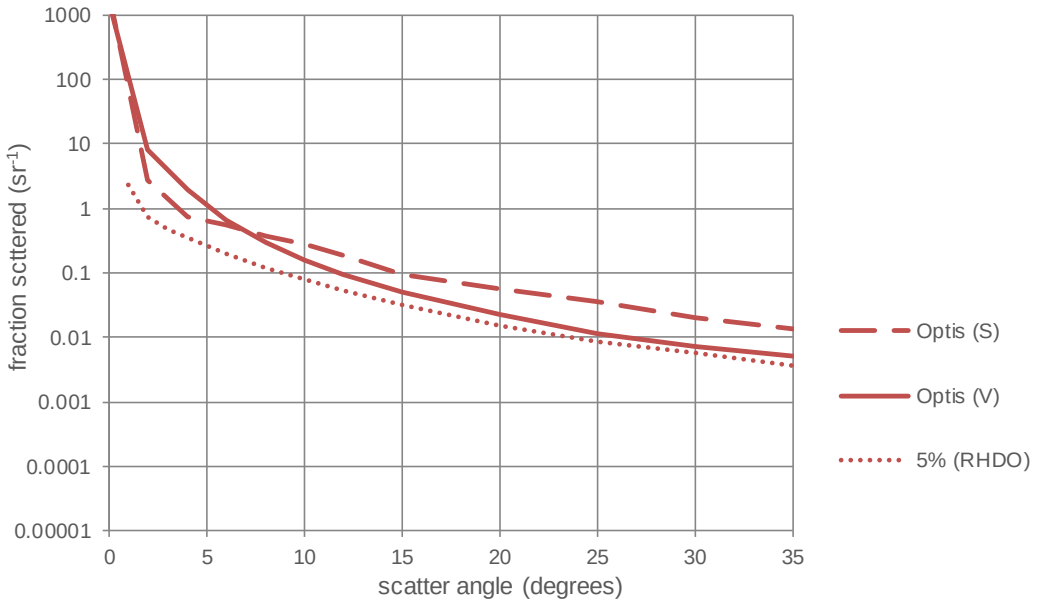

Figure 15. Optis simulation results (OMS4 BSDF file) applied as a surface scatterer (S – dashed line) and a volume scatterer (V – solid line) compared to RHDO measurements for the 5% haze standard (dotted line)

While performing this simulation it was noted that the volume scattering approach provided a better initial correlation; however, it was not as easy to apply a correction factor to the BSDF measurement as in the surface scatter method. When applied as a surface scatter effector, the method for correcting the BSDF measurement involved a simple modification of the transmission and absorption values, which was a simple process and could be performed rapidly. For volume scattering measurements, a mathematical model (Henyey-Greenstein) was applied and the model parameters were adjusted to attempt to improve the fit to the measured data. However, the impact of changing the model parameters on the model output was not intuitive, and this made adjustments difficult.

3.3 Modeling results- Human vision

The luminance of the Regan chart simulation outputs were determined for the letter and background pixels, and the letter contrasts were calculated and compared to the actual measured values. The results were within 0.2% or better of the specified contrasts (Table 1).

Table 1 Regan chart contrast levels, background and letter luminance values from the simulation, calculated model contrast and the contrast error of the model.

Actual contrast (%)	Background luminance ($cd \cdot m^{-2}$)	Letter luminance ($cd \cdot m^{-2}$)	Model contrast (%)	Contrast error (%)
96	105.1	4.3	95.9	-0.1
50	104.9	52.2	50.2	0.2
25	104.8	78.8	24.8	-0.2
11	105.0	93.3	11.1	0.1
4	104.9	100.7	4.0	0.0

The complete assembly model included the haze sample, BAT, and Regan charts. Figure 16 shows the model looking through the BAT aperture at a line on the Regan chart, with the haze sample positioned between the eye and BAT. Using these custom-built components, in conjunction with the Legibility and Visibility tool within OW, it should be possible to simulate the effects on visual performance of viewing the Regan charts through optical samples varying in light scatter characteristics with the BAT glare source present. Figure 17 illustrates a possible output of the model where the field of view of the detector covers the two central letters of the chart. In this illustration, the light has not been scattered but absorbed by a neutral filter, reducing the luminance of both the background and the letters, but having no impact on contrast. In reality, a typical LEP device will affect both the luminance and the contrast of the letters.

The light scatter model was not considered to be a sufficiently accurate and generalizable representation of the laboratory measurements for the validation step, involving comparisons of the modeled results on human vision with experimental data involving human subjects. This task was, therefore, deferred until a more accurate model is available.

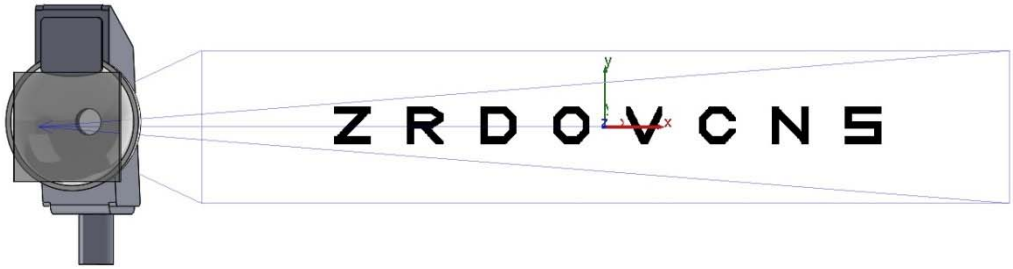

Figure 16. 3D assembly model of a haze sample over the BAT which is pointed at a line of letters on a Regan chart.

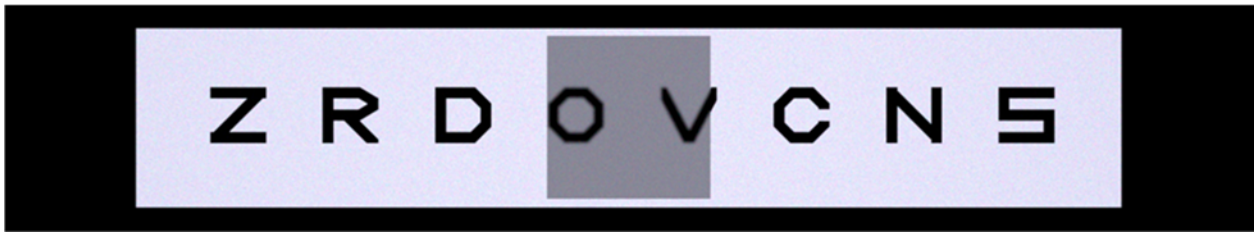

Figure 17. Bitmap image showing simulation result through a neutral filter.

4 SUMMARY

A simple scatterometer was constructed in the RHDO laboratory and used to make scatter measurements for four BYK-Gardner haze-standard samples with 1, 5, 10 and 20% haze. The scatterometer was modified to improve sensitivity, and the scatter measurements repeated. The RHDO lab data were compared with independent BTDF measurements collected using a more sensitive and validated scatterometer and the results compared well. The scatter data were then imported into the OW CAD environment and modified using various built in scatter editors available in the OW lighting and simulation software in an attempt to model the lab measurements accurately. The OW scatter simulations showed a similar trend to the laboratory measurements; however, the simulation produced significantly lower scatter values. While an empirical correction factor could be used to improve the model fit, this process would not be generalizable, and so was not attempted.

The discrepancy between laboratory measurements and the simulation results was determined to primarily be due to the data not conforming to the material file structure, which is specific to OW software construct. However, because of proprietary restrictions imposed on the file structure, it was not possible to import “external” BSDF into the OW simulation. To support the development of a simulation using a BSDF file in OW format, the 5% haze sample was sent to Optis North America to be measured with their internally developed OMS4 measurement system. During the measurement process Optis advised that the OMS4 required a certain level of scattering in order

to produce high fidelity results. It was not specifically designed to measure very low levels of scatter, like that in the 5% haze sample. Two scatter models were used to apply the OMS4 scatter function: a surface scatter model and a volumetric scatter model. These were adjusted with "correction factors" to try to improve the match between the model and the laboratory measurements. The volumetric scattering model matched the laboratory measurements more closely, but was found more difficult to adjust than the surface scatter model.

To support validation of the applicability of the scatter model to human visual performance analysis, a 3D model of the optical set-up used in a study of the effects of optical scatter in the presence of glare on the visual acuity of human observers was developed. The components of the model included the charts from the Regan Contrast Acuity test, the BAT glare source, haze samples, a light detector to simulate the human eye, and a human visibility/legibility tool.

5 RECOMMENDATIONS

To progress this modeling effort, the key step of importing BTDF/BSDF data into the OW modeling and simulation environment needs to be resolved. Incorporating laboratory-measured scatter functions directly or using a scatter tool designed for OW did not prove successful, so alternative approaches need to be considered.

It should be possible to develop an accurate scatter model using optical design software, such a Zemax OpticStudio, and then incorporate this model into the CAD environment. The Zemax OpticStudio suite provides sequential and non-sequential raytracing functionality, and the flexibility for developing optical material files in a user defined format. In addition, Zemax is able to dynamically link to the SW environment. The first step in this process would be to develop a stand-alone scatter model in Zemax that correlates well with the laboratory-measured data. Once this is complete, the Zemax application programming interface can be used to incorporate the Zemax model into the OW environment, and thus allow the human visual performance validation step to proceed. This solution would be expected to provide the most accurate and flexible approach.

Alternatively, as suggested by OW experts, a "brute force" approach could be used. This would involve using a simple scattering file based on specular, Gaussian and Lambertian scattering, and developing an automated optimization algorithm that would be used to adjust their relative contributions to provide a best-fit of the scatter model to the measured data. This approach may be easier in the short-term, but since it is an empirically-based solution, it would be more difficult to generalize to different optical scattering materials.

6 LIST OF ABBREVIATIONS

3D	Three-Dimensional
BAT	Brightness Acuity Tester
BMP	BitMap
BRDF	Bi-directional Reflection Distribution Function
BSDF	Bi-directional Scatter Distribution Function
BTDF	Bi-directional Transmission Distribution Function
CAD	Computer Aided Design
FOV	Field of View
HVL	Human Vision Lab
LEP	Laser Eye Protection
OMS	Optical Material Scanner
OW	OptisWorks
RHDO	711th Human Performance Wing, Airman Systems Directorate, Bioeffects Division, Optical Radiation Bioeffects Branch
RGB	Red, Green and Blue
SW	SolidWorks
TIS	Total Integrated Scatter
UME	User Material Editor
XMP	Extended Image Map

7 REFERENCES

1. Thomas, S.R. (1994). "Aircrew laser eye protection: Visual consequences and mission performance," *Aviat., Space, and Environ. Med., Supplement A*, A108- A115.

2. ASTM –D1003-13. Standard Test Method for Haze and Luminous Transmittance of Transparent Plastics, ASTM International, West Conshohocken, PA.

3. Human Systems Group, United States Air Force. (2005). Performance Specification for the Block 2 Aircrew Laser Eye Protection (ALEP) System; Main body (Unclassified). HGU-APA-01-Block2 ALEP/PS0

4. Marasco PE, Task HL. (1999). The effect on vision of light scatter from HMD visors and aircraft windscreens. Proc. SPIE 3689, Helmet- and Head-Mounted Displays IV.

5. Ghani, N., Dykes, J., Garcia, P., Schmeisser, E., Maier, D., and McLin, L.N. (2001). The Effect of Glare on Regan Contrast Letter Acuity Scores Using Dye-Based Laser Eye Protection. AFRL-HE-BR-TR-2001-0094. USAF Research Laboratory, Brooks City-Base TX 78235.

6. Dykes J, Garcia P, Maier D, McLin L, Ghani N, Schmeisser E, Harrington K. (2004). Quantifying the Effects of Haze in Laser Eye Protection on Regan Contrast Letter Acuity. AFRL-HE-BR-TR-2004-0055. USAF Research Laboratory, Brooks City-Base TX 78235.

7. Kuyk TK, Smith PA, Engler SN, Garcia PV, Brockmeier, WR, Novar BN, Putnam CM, McLin LN. The Effects of Scattered Light from Optical Components on Visual Function. AFRL-HE-FS-TR-2016-0018. USAF Research Laboratory, Ft. Sam Houston, TX 78234.

8. Edmonds, BP and Irvin, G. Personal communication, March 2015.

9. Regan D, Neima D, (1983) Low-contrast letter charts as a test of visual function. Ophthalmology, 90:1192-1200.